# Magnetic Resonance Imaging of Joint Replacements

**Ali M. Naraghi, F.R.C.R.[1] and Lawrence M. White, M.D.[2]**

**ABSTRACT**

An increasing number of joint replacements are being performed annually. Complications of joint arthroplasty are diverse and may involve the hardware as well as osseous and soft tissue components. Although modalities such as conventional radiography and scintigraphy remain the mainstay of radiological investigation, in some cases these traditional methods of imaging may be negative or underestimate the extent of disease. Magnetic resonance imaging (MRI) has been considered of limited benefit following arthroplasty because of severe image degradation caused by metallic components. However, with modification of pulse sequences, artifact reduction and improved visualization of periprosthetic tissues are achievable, enabling a comprehensive assessment of articular and nonarticular pathologies. The common artifacts in the presence of orthopedic hardware, optimization of pulse sequences to minimize metal-related artifacts, and the clinical uses of MRI following joint replacement, particularly with regard to total hip arthroplasty, total knee arthroplasty, and shoulder arthroplasty, are reviewed.

**KEYWORDS:** Magnetic resonance imaging, artifacts, arthroplasty

Approximately 636,000 arthroplasties are performed annually in the United States[1] and this rate is increasing by 5% per annum.[2] The vast majority of these consist of total hip and total knee replacements. Improvements in component design and surgical techniques have not only yielded a reduction in complication rates related to joint replacements[3–5] but also resulted in an alteration in the relative frequency of these complications.[6] Nevertheless, a small but significant proportion of patients present with residual or recurrent symptoms, typically of pain or instability after arthroplasty, which can be a difficult challenge to evaluate and treat.

Annual or biennial clinical and radiographic evaluation is the most commonplace mode of follow-up subsequent to joint arthroplasty.[2] In the presence of clinical symptoms or radiographic abnormalities, further radiological and laboratory investigations are often initiated. Traditionally, radiological assessment has consisted of a combination of stress radiography, nuclear scintigraphy, arthrography, and more recently computed tomography (CT) and ultrasonography.[7,8]

Magnetic resonance imaging (MRI) has not been typically used in the evaluation of joint replacement as a consequence of problems related to metal susceptibility artifacts. However, with the development of techniques to reduce susceptibility artifacts around metallic implants, there is now a growing body of work that demonstrates the value of MRI in the presence of orthopedic hardware. With its exquisite soft tissue contrast, direct multiplanar capabilities, lack of ionizing radiation, and the ability to demonstrate articular and nonarticular pathology, MRI is emerging as a valuable

An Update on Imaging of Joint Reconstructions; Editors in Chief, David Karasick, M.D., Mark E. Schweitzer, M.D.; Guest Editor, Theodore T. Miller, M.D. *Seminars in Musculoskeletal Radiology*, Volume 10, Number 1, 2006. Address for correspondence and reprint requests: Lawrence M. White, M.D., Mount Sinai Hospital and University Health Network, Department of Diagnostic Imaging, 600 University Avenue, Toronto, Ontario, Canada, M5G 1X5. [1]Royal London Hospital, Department of Diagnostic Imaging, London, United Kingdom; [2]Mount Sinai Hospital and University Health Network, Department of Diagnostic Imaging, Toronto, Ontario, Canada.  1089-7860,p;2006,10,01,098,106,ftx,en;smr00389x.

tool in assessment of arthroplasties to elucidate the cause of symptoms in the setting of normal radiographs and to further delineate and characterize pathology demonstrable on routine imaging.

## OPTIMIZATION OF IMAGE QUALITY IN PRESENCE OF METALLIC HARDWARE

Magnetic susceptibility refers to the tendency of a substance to become magnetized when exposed to an external magnetic field. The degree of magnetization is proportional to the applied magnetic field[9] and is an inherent property of a substance. When objects of different magnetic properties are placed within an external magnetic field, local field inhomogeneities result, distorting the local gradient fields. As a homogeneous magnetic field and gradients are a prerequisite for MRI imaging, any such distortion results in production of imaging artifacts. The more strongly magnetism is induced in a metal component, the greater the degree of artifacts encountered. Titanium-based prostheses, because of their reduced ferromagnetic characteristics, result in less distortion of the local fields than stainless steel or cobalt chromium implants and therefore produce comparatively diminished image degradation.[10–15]

Although as imagers we have no control over the type of prosthesis employed or its ferromagnetic tendencies, by manipulation of imaging parameters the resultant artifacts can be minimized. Ideally, any such measures should have no deleterious impact on acquisition time, patients' comfort, or signal-to-noise ratio and should be easily achievable on most commercial units.

Metal-induced artifacts are composed of intravoxel dephasing, misregistration, diffusion-related signal loss, and slice thickness variation.[16]

Intravoxel dephasing is most prominent and the primary cause of signal loss visualized in gradient-recall echo (GRE) imaging. Magnetic field inhomogeneities caused by metallic hardware accentuate the loss of phase coherence of spins and therefore result in signal loss. Spin echo (SE) and fat spin echo (FSE) pulse sequences utilize single or multiple 180-degree refocusing pulses to recover transverse signal loss induced by metal-related distortion of the local magnetic field. In contrast, GRE imaging lacks a 180-degree pulse and consequently the signal loss is not recovered. Furthermore, this signal loss is greater with longer echo times (TEs).[15,17,18] As a result, GRE sequences suffer from severe image degradation and signal voids and should be avoided in the presence of bulk orthopedic hardware.

Misregistration is the principal artifact encountered in SE and FSE imaging. This is manifest as geometric areas of signal alteration in the frequency-encoding direction, and thus the direction of the frequency-encoding gradient can be selected to direct the misregistration artifact away from the area of interest.[10,11,14,19,20] Its dimension is directly proportional to the magnitude of the local field inhomogeneities. As the distortion of local magnetic fields in the presence of a given ferromagnetic material is proportional to the applied magnetic field, misregistration artifacts tend to be more severe at higher main magnetic field strengths.[21,22] However, lower magnetic field strengths suffer from a poorer signal-to-noise ratio.[23] Misregistration artifacts are also inversely proportional to the frequency-encoding gradient strength. For a given field of view, a broader receiver bandwidth results in a higher gradient field strength, thus diminishing this type of artifact.[15] This also results in a poorer signal-to-noise ratio, which may necessitate a compensatory increase in the number of excitations for acquisitions of similar image quality.[15,24] Artifacts also tend to be greatest when metallic components are aligned perpendicular to the main magnetic field ($B_o$), progressively decreasing as the angle between the long axis of the component and $B_o$ is reduced.[9,10,12,25] This partly accounts for the reduced image degradation around the stems of femoral components of total hip arthroplasties and humeral components of shoulder arthroplasties imaged in closed configuration high-field MRI systems where $B_o$ is aligned along the bore axis, parallel to the long axis of the prosthesis stem.

Therefore, maneuvers demonstrated to minimize misregistration artifact include broadening of receiver bandwidth and using a higher frequency-encoding strength,[15,24,26] orienting the long axis of metallic hardware along $B_o$, orienting the frequency-encoding direction along the longitudinal axis of the prosthesis or away from the anatomic region of interest, and utilizing a lower field strength magnet.

Bulk ferromagnetic implants also result in increased spin dephasing in randomly moving water molecules. This diffusion-related signal loss is not completely recoverable by the 180-degree refocusing pulse employed in SE imaging[15] and is accentuated by long TE acquisitions.[16] This can be partly overcome by FSE sequences, which make use of multiple 180-degree refocusing pulses. With shorter true echo times than the effective echo time, spins refocus at a faster interval and with less time for dephasing to occur, thereby reducing diffusion-related signal intensity loss and causing an increase in signal intensity. The time between applications of sequential 180-degree pulses has a critical effect on preservation of signal in FSE imaging.[11,27]

Distortion of the local magnetic field induced by ferromagnetic implants additionally result in variations in the frequency-selective slice excitation profiles by altering the isomagnetic lines within the imaging volume.[28] The maximum change in the magnetic field occurs adjacent to regions where magnetic field lines emerge from the implant. This is manifest as variation in the slice thickness adjacent to metal hardware and is

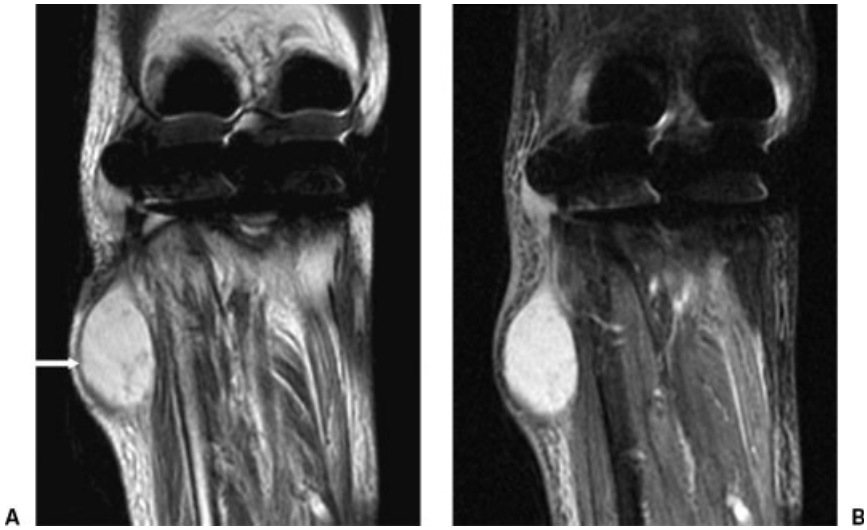


**Figure 1** Coronal T2-weighted fast spin-echo image with fat saturation (A) (TR/TE, 3500/90 milliseconds; ETL, 12), after right total knee arthroplasty, demonstrates a focal cystic collection along the lateral aspect of the proximal calf (arrow). Inhomogeneity of fat saturation is seen with spectral fat suppression used in the presence of bulk metallic hardware. Corresponding coronal STIR image (B) (TR/TE, 4400/16 milliseconds; TI 150 milliseconds) demonstrates more uniform fat suppression.

dependent on the geometry of the component, being greatest adjacent to spherical and nonuniform structures such as the head of the femoral prosthesis or the acetabular component.[28] Reduction in slice thickness and an increase in matrix size, by reducing the voxel size, maximize spatial resolution and assist in minimizing the conspicuity of the area affected by signal loss and geometric distortion.[15] This may be achieved without time penalties by increasing the number of pixels in the frequency-encoding direction of the slice. This type of artifact may be eradicated by utilizing phase encoding of slice selection as employed in three-dimensional (3D) techniques. This has the benefit of being immune to the local magnetic field inhomogeneity but suffers from long acquisition times.

Spectral fat saturation pulse sequences, commonly utilized in musculoskeletal MRI, are heavily dependent on a uniform magnetic field, enabling the precise differences in the resonance frequencies of hydrogen protons in fat and water to be exploited by delivering a radiofrequency (RF) suppression pulse matching the spectral frequency of fat. Local distortions of magnetic fields around ferromagnetic substances alter the spectral frequencies of fat and water in the region and ineffective fat suppression or paradoxical water suppression may ensue. Short tau inversion recovery (STIR) pulse sequences are less susceptible to such local inhomogeneity (Fig. 1) and are the preferred method of fat suppression in the presence of metallic hardware despite a poorer signal-to-noise ratio.[29] The Dixon technique is a further method of water-fat separation[30] but becomes inaccurate in the presence of $B_0$ inhomogeneities.[31] The three-point Dixon technique is a modifications of the original technique using multiple data sets, allowing effective water-fat separation even in the presence of $B_0$ inhomogeneity and at low magnetic field strengths. Although it originally suffered from long acquisition times, problems with patient movement, and the need for lengthy image reconstruction algorithms, further modifications have addressed these drawbacks and have also enabled generation of T1- and FSE T2-weighted three-point Dixon images.[31–35] However, the results of these techniques in the presence of bulk metallic hardware have not been documented.

View angle tilting has also been utilized in an attempt to reduce metal-induced artifacts.[12–14,26] This technique uses a modified SE pulse sequence whereby an additional slice selection gradient is applied during signal acquisition to reduce geometric distortion. This additional gradient has the same amplitude as the normal slice selection gradient but is applied at the time of the read gradient,[26] thus ensuring that the spins precess in a narrow frequency band during readout to avoid image distortion. This technique has been used with[24] and without[26] other concurrent measures to reduce artifact, namely broadening the RF bandwidth and also increasing the section-selection and read gradients. The main drawback of this modification has been blurring of the image and a shift in the image field of view. The latter can be corrected by means of a prescan calculation but requires knowledge of gradient magnitudes and adds to the total scanning time.

In vitro studies using single-point imaging (SPI) techniques, a form of solid-state MRI technology, have also been examined in the presence of orthopedic prostheses. This form of imaging is immune to misregistration artifacts by virtue of collecting one point of free induction decay immediately after excitation, before signal from solid elements dephases. This technique requires large gradient amplitudes of high spatial resolution and additionally the step-by-step filling of the k-space results in long scanning times, issues that have been addressed by modification of gradient application and k-space filling techniques. Using these approaches, exquisite in vitro images of metallic

**Table 1 Methods of Artifact Reduction in the Presence of Metallic Hardware**

| Artifact | Artifact Reduction Modification |
|---|---|
| Intravoxel dephasing | Use SE and FSE sequences in lieu of GRE. |
| Misregistration | Broaden receiver bandwidth |
| | Use higher frequency-encoding strength. |
| | Orient long axis of implant with $B_o$. |
| | Orient frequency-encoding along long axis of implant. |
| | Use lower magnetic field strength. |
| | View angle tilting. |
| Diffusion-related signal loss | Use FSE and short TE sequences. |
| | Reduce interecho spacing. |
| Slice thickness variation | Reduce slice thickness. |
| | Increase matrix size. |
| | Use 3D techniques. |
| Inhomogeneous fat saturation | Use STIR instead of spectral fat saturation. |
| | Use modified three-point Dixon technique. |

prostheses completely free of distortion have been achieved[36] (Table 1).

## TOTAL HIP ARTHROPLASTY

Annually, approximately 180,000 total hip arthroplasties are performed in the United States[1] and of these 20% consist of revision arthroplasties. Furthermore, the proportion of revision arthroplasties in relation to the primary procedure is increasing.

Complication of hip arthroplasty and causes of recurrent symptoms are numerous and can be classified as intrinsic and extrinsic.[7] Intrinsic complications, some of which may lead to revision surgery, include mechanical loosening, polyethylene wear and osteolysis, infection, prosthesis failure and periprosthetic fracture, occult instability, heterotopic ossification, bursitis, and tendinopathy. In particular, foreign body granulomatosis or osteolysis is emerging as an increasingly important and common complication of joint replacements.[37] Extrinsic causes include lumbar spine disease, nerve injury, irritation, and neuroma formation.

Highly variable sensitivities and specificities have been obtained for detection of the preceding complications, in particular aseptic loosening, infection, and osteolysis, using conventional radiography, nuclear scintigraphy, and arthrography. The sensitivity and specificity of MRI in the setting of symptomatic hip arthroplasty have not been fully evaluated, but investigators have demonstrated the ability of MRI to detect radiographically occult pathology and to evaluate radiographic abnormalities in the setting of hip replacements.

In a study of eight patients referred for MRI for assessment of pain and clinical prosthesis failure, in the presence of normal radiographs, scintigrams, and arthrograms with joint aspiration, no cause for pain was demonstrated in six cases.[38] In two cases, however, gluteal avulsion from the greater trochanter was demonstrated. In this study, T1- and FSE T2-weighted sequences were used in conjunction with STIR images, but the authors do not comment regarding the visibility of periprosthetic osseous structures or the use of other methods of artifact reduction.

Other investigators have also examined the role of MRI in evaluation of patients with trochanteric pain following total hip replacement.[39] These investigators have demonstrated that signal and diameter changes of gluteal muscles as well as bursal fluid collections may be seen in asymptomatic individuals following total hip arthroplasty using a lateral transgluteal approach, whereas tendon defects and fatty atrophy of gluteus medius and the posterior half of gluteus minimus are rarely encountered in asymptomatic cases.

In another retrospective evaluation of 50 cases of total hip arthroplasty examined by MRI, multiple findings not evident with plain radiographs were demonstrated. These included osteolysis, bursitis, and scarring.[23]

In a prospective study of 14 hips with symptoms or radiographic abnormalities referred for consideration of revision arthroplasty, MRI with modified parameters to minimize artifact demonstrated periprosthetic abnormalities in 11 cases.[15] The abnormalities demonstrated included mechanical loosening (2 cases), granulomatosis (8 cases), and infection (1 case). In all the cases in which surgical correlation was available, MRI established the correct diagnosis including a case of periprosthetic fracture in the setting of mechanical loosening. In this study, loosening was demonstrated as a nonenhancing linear area of low T1 signal and high T2 signal, paralleling the femoral prosthesis. Cases of osteolysis manifested as localized periprosthetic intraosseous mass lesions with low signal on T1 acquisitions and low to intermediate signal on T2 pulse sequences with heterogeneity of

**Figure 2** Conventional radiograph (A) of a patient following right total hip arthroplasty demonstrating focal destructive lesion of the medial femoral cortex (arrow) with faint mineralization referred for imaging evaluation as possible metastatic deposit. Coronal STIR image (B) (TR/TE, 4200/15 milliseconds; TI 150 milliseconds) demonstrates a lobulated lesion (arrow) causing cortical destruction. Axial fast spin-echo T1-weighted images (TR/TE, 660/9 milliseconds; ETL 6) before (C) and after (D) intravenous gadolinium exhibit a mass of low T1 signal with peripheral rim enhancement (arrow) with no significant central enhancement consistent with an avascular mass. Biopsy revealed histological evidence of small particle disease.

internal architecture. Following intravenous gadolinium, peripheral and patchy internal enhancement was observed. The case of infection was observed in the presence of a soft tissue fluid collection. Visualization of tissues about the femoral prosthesis was satisfactory in all cases (Fig. 2), but adequate visualization of periacetabular tissues was achieved in only 36%.

The role of MRI in evaluating the extent of osteolysis to plan revision arthroplasty and the need for bone grafting has been assessed.[40] The authors of this investigation found that in a population of 28 hips, of which there was surgical correlation in 15, radiography underestimated the extent of osteolysis as compared with MRI. MRI also allows exact localization of areas affected by osteolysis (Fig. 3). In addition, cases of soft tissue deposits with similar signal intensity to the areas of osteolysis were demonstrated on MRI imaging. Foci of osteolysis were found to consist of well-demarcated areas of intermediate signal intensity with a hypointense rim separating it from the adjacent marrow. This is in contrast to areas of infection, which were depicted as ill-defined areas of high signal intensity with adjacent marrow edema. In 24 cases, synovitis with particulate matter, similar in signal intensity to the osteolytic deposits in bone, was also identified. Other findings included heterotopic ossification, insufficiency fractures of the sacrum and pubic rami, and greater trochanteric bursitis.

Component failure has also been demonstrated using MRI.[41] A patient with thigh pain, normal radiographs, CT scan, joint aspirate, and subtle tracer uptake on bone scan was investigated by MRI for further elucidation of ongoing symptoms. MRI with artifact

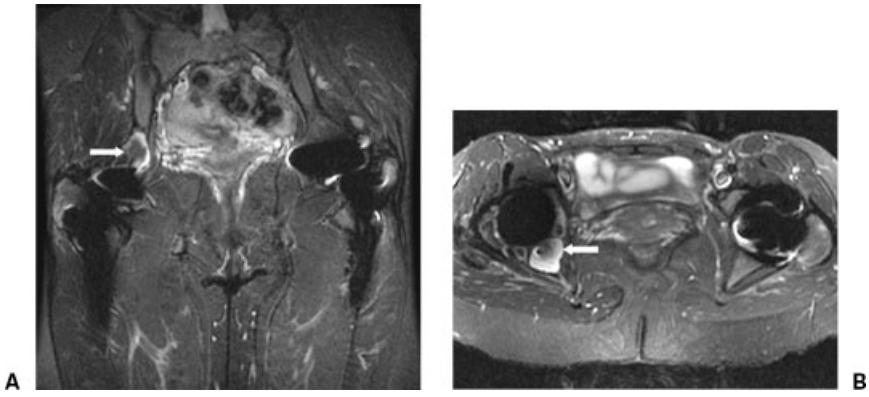

**Figure 3** Coronal (A) and axial (B) STIR images (TR/TE, 4400/22 milliseconds; TI 150 milliseconds) of the right total hip arthroplasty demonstrate well-circumscribed focal lobulated areas of intraosseous increased T2-weighted signal change involving the medial and posterior walls of the acetabulum as well as the supra-acetabular region (arrows) consistent with osteolysis.

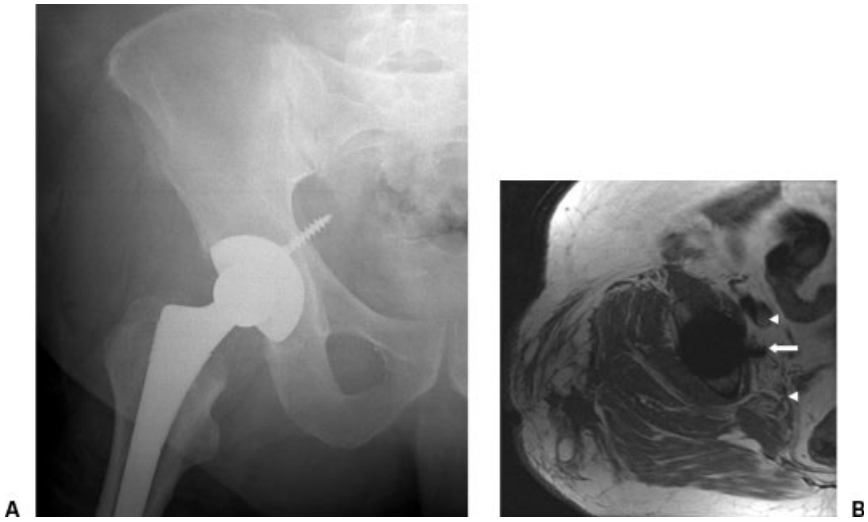

**Figure 4** Immediate postoperative conventional radiograph (A) following noncemented total hip arthroplasty illustrates protrusion of the acetabular screw into the pelvis. The patient complained of severe radiating pain. MRI was performed to investigate the location of the screw in relation to the sciatic nerve. Axial fast spin-echo T1-weighted image (B) (TR/TE, 450/7 milliseconds; ETL 6) shows the screw (arrow) to be remote from the sciatic nerve and external iliac vessels (arrowheads). Postsurgical changes are noted lateral to the gluteal muscles.

reduction parameters identified a fracture of the tensile aspect of the femoral component, confirmed at surgery.

Other investigators have demonstrated the utility of low-field-strength MRI imaging of total hip arthroplasty.[42] The authors of this study examined the periprosthetic regions of femoral implants in 22 cases and categorized periprosthetic signal intensity into three types. Type I pattern consisted of high signal intensity on STIR images with no gadolinium enhancement on T1-weighted sequences. Type II demonstrated high signal intensity on STIR with gadolinium enhancement on T1-weighted images. Type III pattern exhibited no contrast enhancement and normal signal intensity on STIR images. MRI findings were assessed against radiographic and surgical findings. The authors concluded that type I and II patterns were associated with focal or nonfocal lucency, an unstable stem, and periprosthetic fibrosis or granulomatosis, whereas type III pattern was associated with normal radiographic appearances and a stable stem, especially if Gruen zones 3 and 5 demonstrated this signal pattern simultaneously. However, zones with type I and type II signal intensity were also visualized in three cases with stable prostheses at surgery.

MRI may also be used in the immediate postoperative period when there is concern regarding immediate complications such as hardware positioning (Fig. 4).

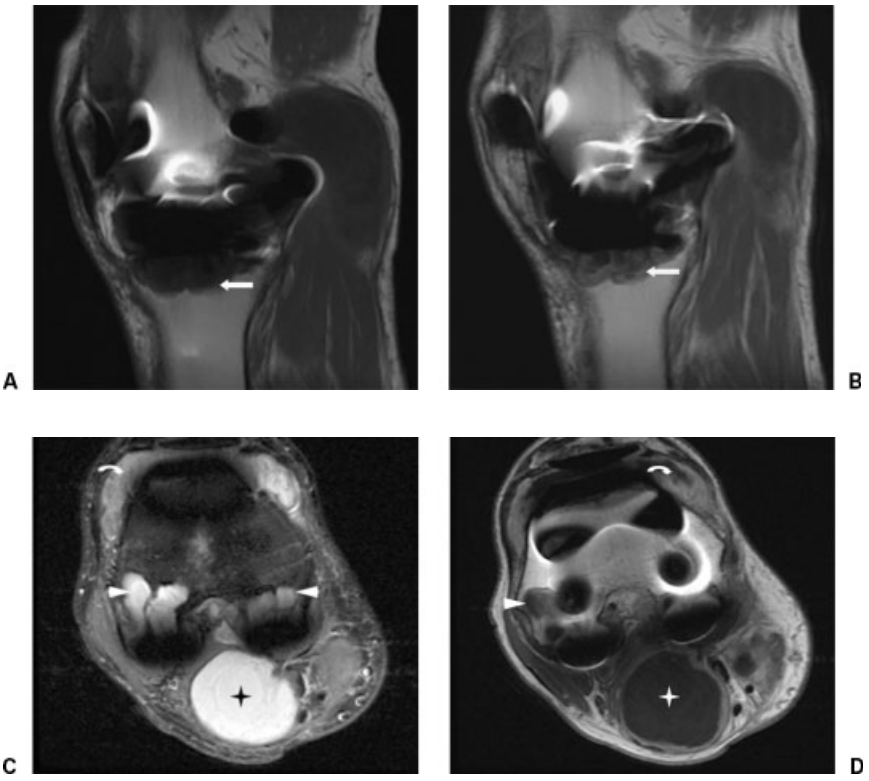

**Figure 5** Sagittal pre- (A) and postgadolinium (B) fast spin-echo T1 (TR/TE, 550/7 milliseconds; ETL 6), axial STIR (C) (TR/TE, 3800/15 milliseconds; TI 150 milliseconds) and axial postgadolinium fast spin-echo T1-weighted (D) (TR/TE, 550/7 milliseconds; ETL 6) images of total knee arthroplasty with patellar resurfacing illustrating lobulated enhancing tissue (arrow) at the base of the tibial tray and the posterior aspect of the femoral condyles (arrowheads) consistent with osteolysis. Extensive synovitis of the suprapatellar pouch (curved arrow) and peripheral enhancement of a large popliteal cyst (star) are also noted.

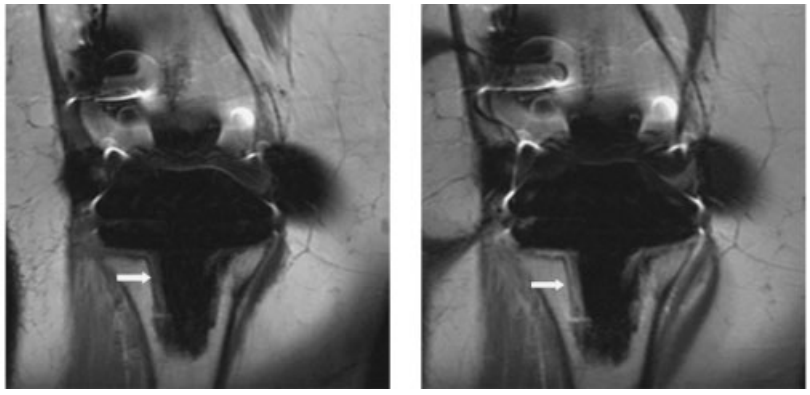


**Figure 6** Coronal fast spin-echo T1-weighted images (TR/TE, 600/7 milliseconds; ETL 6) before (A) and after (B) intravenous gadolinium show nonfocal linear enhancement (arrow) paralleling the prosthetic-bone interface of the tibial component of a total knee arthroplasty interpreted as loosening. At surgery the tibial component was loose and there was no evidence of infection or osteolysis on laboratory analysis.

## TOTAL KNEE ARTHROPLASTY

The total number of knee arthroplasties, including primary and revision surgery, is approximately 327,000 per year.[1] Articular causes of pain after knee arthroplasty, as in the case of hip arthroplasty, include loosening, periprosthetic osteolysis, instability, component failure, infection, and particulate-induced synovitis. Other causes of symptoms encountered following knee arthroplasty include extensor mechanism failure, patellar maltracking, patellar clunk syndrome, tendinopathy, bursitis, popliteus tendon dysfunction, and cutaneous neuromas.[8] Traditional methods of imaging have limitations similar to those encountered following hip arthroplasty. In some cases no articular or nonarticular causes are identified, the so-called mystery knee.[43] The most common causes for early failure within the first 5 years include infection, instability, and patellofemoral disorders; polyethylene wear, aseptic loosening, and osteolysis are less common.[44] Overall, however, polyethylene wear, loosening, and instability are the leading causes of revision arthroplasty of the knee.[45]

Studies of the utility of MRI following knee arthroplasty are scarce. In general, image degradation in the knee is more severe than in the hip owing to the more complex geometry of the components. The only sizable study to date retrospectively reviewed MRI findings in 46 knees.[46] FSE and STIR images with broadened bandwidths were acquired and the authors were able to visualize satisfactorily periprosthetic soft tissues including the extensor mechanism, collateral ligaments, and the popliteus in all cases. They also noted that with the more recent examinations, as a result of higher bandwidths and modifications of interecho spacing, visualization was further improved, enabling better assessment of soft tissues, metal-bone interface, and the polyethylene spacer. Demonstrable pathologies consisted of osteolysis in seven cases, none of which were identified on conventional radiographs; collateral ligament tears in five cases; and cases of quadriceps, patellar tendon, iliotibial band, and medial retinacular tears. This study clearly identified advantages of MRI in the global assessment of the knee (Figs. 5–8) by identifying both osseous and soft tissue abnormalities, which are often not easily apparent with other imaging techniques.

## TOTAL SHOULDER ARTHROPLASTY

Shoulder arthroplasty is the third most common arthroplasty performed, but there are only 8000 cases per annum in the United States and a proportion of these

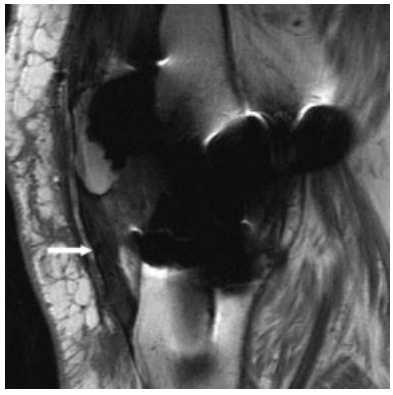

**Figure 7** Sagittal intermediate-weighted fast spin-echo image (TR/TE, 2150/30 milliseconds; ETL 8) of total knee arthroplasty displays thickening and increased signal within the patellar tendon (arrow) in keeping with patellar tendinopathy.

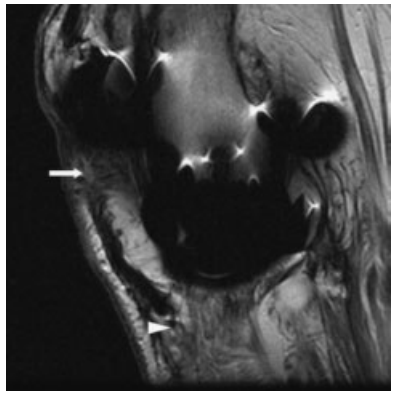

**Figure 8** Sagittal T2-weighted fast spin-echo image (TR/TE, 3200/90 milliseconds; ETL 12) of total knee arthroplasty illustrates complete tears of the proximal (arrow) and distal (arrowhead) patellar tendon.

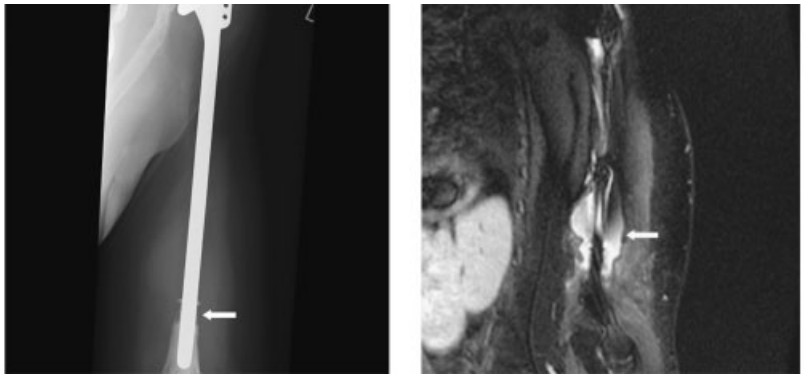

**Figure 9** Conventional radiograph (A) of long-stem humeral hemiarthroplasty for reconstruction after proximal humeral resection for treatment of prior osteosarcoma demonstrates localized osseous resorption surrounding the distal humeral stem (arrow). Coronal STIR image (B) (TR/TE, 4200/15 milliseconds; TI 150 milliseconds) through this region demonstrates a localized fluid collection (arrow) with no evidence of recurrence. Aspiration revealed infection.

consist of hemiarthroplasties.[1] The most common complication following total shoulder arthroplasty is rotator cuff tear. Other complications include instability, malpositioning, infection, and loosening. Complications of hemiarthroplasty include glenoid cartilage loss and nonunion of tuberosities in cases of fractures. Although plain radiographic evaluation may facilitate the diagnosis of malalignment, the soft tissue and cartilaginous abnormalities are detected only in late cases.

MRI of the postarthroplasty shoulder can result in relatively increased image degradation as the shoulder is not located within the center of the magnetic field, where there is greater homogeneity, but lies to the periphery, where the magnetic field is more inhomogeneous. Furthermore, the geometry of the humeral head component can result in severe artifact.

In a review of 42 cases, of which there was surgical correlation in 21, MRI correctly demonstrated rotator cuff tears in 10 of 11 cases.[47] Identification of cuff tears is crucial in this group of patients as glenoid component loosening, which can affect 30 to 60% of cases, is often due to ascension of the humeral head as a result of cuff tears and dysfunction.[48] The most common lesion identified was a full-thickness tear of subscapularis. Other abnormalities revealed included synovitis, heterotopic ossification, infection with a localized fluid collection (Fig. 9), anteversion of the humeral head, and glenoid loosening, although in the experience of the authors the presence of periprosthetic signal alone did not correlate with a loose glenoid component. It was also noted that visualization of the lesser tuberosity and the biceps tendon was suboptimal.

## SUMMARY

Simple modifications of commonly used pulse sequences can result in dramatic improvements in the severity of metal-related artifacts at MRI imaging and enhance visualization of periprosthetic tissues. This can be accomplished without a substantial penalty in terms of acquisition time. This has enabled MRI to be of increasing benefit as a problem-solving tool in symptomatic cases with negative findings on routine imaging and in cases in which radiographic abnormalities require further characterization with regard to extent and etiology.

## REFERENCES


1. American Academy of Orthopaedic Surgeons. Arthroplasty and Total Joint Replacement Procedures 1991–2000. Available at http://www.aaos.org/wordhtml/research/arthropl.htm. Accessed October 12, 2004
2. Teeny SM, York SC, Mesko JW, Rea RE. Long-term follow-up care recommendations after total hip and knee arthroplasty. J Arthroplasty 2003;18:954–962
3. Eustace S, Shah B, Mason M. Imaging orthopedic hardware with an emphasis on hip prostheses. Orthop Clin North Am 1998;29:67–84
4. Chandler HP, Reineck FT, Wixson RL. Imaging orthopedic hardware with an emphasis on hip prostheses. Total hip replacement in patients younger than thirty years old. A five-year follow-up study. J Bone Joint Surg Am 1981;63:1426–1434
5. Weissman BN. Current topics in the radiology of joint replacement surgery. Radiol Clin North Am 1990;28:1111–1134
6. Callaghan JJ, O'Rourke MR, Saleh KJ. Why knees fail: lessons learned. J Arthroplasty 2004;19(4 Suppl 1):31–34
7. Bozic KJ, Rubash HE. The painful total hip replacement. Clin Orthop Relat Res 2004;420:18–25
8. Dennis DA. Evaluation of painful total knee arthroplasty. J Arthroplasty 2004;19(4 Suppl 1):35–40
9. Guermazi A, Miaux Y, Zaim S, Peterfy CG, White D, Genant HK. Metallic artefacts in MR imaging: effects of main field orientation and strength. Clin Radiol 2003;58:322–328
10. Suh JS, Jeong EK, Shin KH, et al. Minimizing artifacts caused by metallic implants at MR imaging: experimental and clinical studies. AJR Am J Roentgenol 1998;171:1207–1213
11. Eustace S, Jara H, Goldberg R, et al. A comparison of conventional spin-echo and turbo spin-echo imaging of soft tissues adjacent to orthopedic hardware. AJR Am J Roentgenol 1998;170:455–458
12. Ganapathi M, Joseph G, Savage R, Jones AR, Timms B, Lyons K. MRI susceptibility artefacts related to scaphoid screws: the effect of screw type, screw orientation and imaging parameters. J Hand Surg [Br] 2002;27:165–170
13. Laakman RW, Kaufman B, Han JS, et al. MR imaging in patients with metallic implants. Radiology 1985;157:711–714

14. Petersilge CA, Lewin JS, Duerk JL, Yoo JU, Ghaneyem AJ. Optimizing imaging parameters for MR evaluation of the spine with titanium pedicle screws. AJR Am J Roentgenol 1996;166:1213–1218
15. White LM, Kim JK, Mehta M, et al. Complications of total hip arthroplasty: MR imaging—initial experience. Radiology 2000;215:254–262
16. White LM, Buckwalter KA. Technical considerations: CT and MR imaging in the postoperative orthopedic patient. Semin Musculoskelet Radiol 2002;6:5–17
17. Czervionke LF, Daniels DL, Wehrli FW, et al. Magnetic susceptibility artifacts in gradient-recalled echo MR imaging. AJNR Am J Neuroradiol 1988;9:1149–1155
18. Tien RD, Buxton RB, Schwaighofer BW, Chu PK. Quantitation of structural distortion of the cervical neural foramina in gradient-echo MR imaging. J Magn Reson Imaging 1991;1:683–687
19. Tormanen J, Tervonen O, Koivula A, Junila J, Suramo I. Image technique optimization in MR imaging of a titanium alloy joint prosthesis. J Magn Reson Imaging 1996;6:805–811
20. Ludeke KM, Roschmann P, Tischler R. Susceptibility artefacts in NMR imaging. Magn Reson Imaging 1985;3: 329–343
21. Arbogast-Ravier S, Gangi A, Choquet P, Brunot B, Constantinesco A. An in vitro study at low field for MR guidance of a biopsy needle. Magn Reson Imaging 1995;13: 321–324
22. Jensen JH, Chandra R. Strong field behavior of the NMR signal from magnetically heterogeneous tissues. Magn Reson Med 2000;43:226–236
23. Sofka CM, Potter HG. MR imaging of joint arthroplasty. Semin Musculoskelet Radiol 2002;6:79–85
24. Olsen RV, Munk PL, Lee MJ, et al. Metal artifact reduction sequence: early clinical applications. Radiographics 2000;20: 699–712
25. Frazzini VI, Kagetsu NJ, Johnson CE, Destian S. Internally stabilized spine: optimal choice of frequency-encoding gradient direction during MR imaging minimizes susceptibility artifact from titanium vertebral body screws. Radiology 1997;204:268–272
26. Viano AM, Gronemeyer SA, Haliloglu M, Hoffer FA. Improved MR imaging for patients with metallic implants. Magn Reson Imaging 2000;18:287–295
27. Tartaglino LM, Flanders AE, Vinitski S, Friedman DP. Metallic artifacts on MR images of the postoperative spine: reduction with fast spin-echo techniques. Radiology 1994; 190:565–569
28. Bakker CJ, Bhagwandien R, Moerland MA, Fuderer M. Susceptibility artifacts in 2DFT spin-echo and gradient-echo imaging: the cylinder model revisited. Magn Reson Imaging 1993;11:539–548
29. Czerny C, Krestan C, Imhof H, Trattnig S. Magnetic resonance imaging of the postoperative hip. Top Magn Reson Imaging 1999;10:214–220
30. Dixon WT. Simple proton spectroscopic imaging. Radiology 1984;153:189–194
31. Moriguchi H, Lewin JS, Duerk JL. Dixon techniques in spiral trajectories with off-resonance correction: a new approach for fat signal suppression without spatial-spectral RF pulses. Magn Reson Med 2003;50:915–924
32. Rybicki FJ, Chung T, Reid J, Jaramillo D, Mulkern RV, Ma J. Fast three-point Dixon MR imaging using low-resolution images for phase correction: a comparison with chemical shift selective fat suppression for pediatric musculoskeletal imaging. AJR Am J Roentgenol 2001;177: 1019–1023
33. Wohlgemuth WA, Roemer FW, Bohndorf K. Short tau inversion recovery and three-point Dixon water-fat separation sequences in acute traumatic bone fractures at open 0.35 tesla MRI. Skeletal Radiol 2002;31:343–348
34. Ma J, Singh SK, Kumar AJ, Leeds NE, Zhan J. T2-weighted spine imaging with a fast three-point Dixon technique: comparison with chemical shift selective fat suppression. J Magn Reson Imaging 2004;20:1025–1029
35. Huegli RW, Tirman PF, Bonel HM, et al. Use of the modified three-point Dixon technique in obtaining T1-weighted contrast-enhanced fat-saturated images on an open magnet. Eur Radiol 2004;14:1781–1786
36. Ramos Cabrer P, van Duynhoven JPM, Van der Toorn A, Nicolay K. MRI of hip prostheses using single-point methods: in vitro studies towards the artifact-free imaging of individuals with metal implants. Magn Reson Imaging 2004;22:1097–1103
37. Tigges S, Stiles RG, Roberson JR. Complications of hip arthroplasty causing periprosthetic radiolucency on plain radiographs. AJR Am J Roentgenol 1994;162:1387–1391
38. Twair A, Ryan M, O'Connell M, Powell T, O'Byrne J, Eustace S. MRI of failed total hip replacement caused by abductor muscle avulsion. AJR Am J Roentgenol 2003;181: 1547–1550
39. Pfirrmann C, Zanetti M, Dora C, Hodler J. MR imaging of abductor tendons and muscles after total hip arthroplasty in asymptomatic and symptomatic patients. Presented at Annual Meeting of the Radiological Society of North America (SSK24–06); December 1, 2004; Chicago, IL
40. Potter HG, Nestor BJ, Sofka CM, Ho ST, Peters LE, Salvati EA. Magnetic resonance imaging after total hip arthroplasty: evaluation of periprosthetic soft tissue. J Bone Joint Surg Am 2004;86:1947–1954
41. Cook SM, Pellicci PM, Potter HG. Use of magnetic resonance imaging in the diagnosis of an occult fracture of the femoral component after total hip arthroplasty. A case report. J Bone Joint Surg Am 2004;86:149–153
42. Sugimoto H, Hirose I, Miyaoka E, et al. Low-field-strength MR imaging of failed hip arthroplasty: association of femoral periprosthetic signal intensity with radiographic, surgical, and pathologic findings. Radiology 2003;229:718–723
43. Vince KG. Why knees fail. J Arthroplasty 2003;18(3, Suppl 1): 39–44
44. Fehring TK, Odum S, Griffin WL, Mason JB, Nadaud M. Early failures in total knee arthroplasty. Clin Orthop Relat Res 2001;392:315–318
45. Sharkey PF, Hozack WJ, Rothman RH, Shastri S, Jacoby SM. Insall Award paper. Why are total knee arthroplasties failing today? Clin Orthop Relat Res 2002;404:7–13
46. Sofka CM, Potter HG, Figgie M, Laskin R. Magnetic resonance imaging of total knee arthroplasty. Clin Orthop Relat Res 2003;406:129–135
47. Sperling JW, Potter HG, Craig EV, Flatow E, Warren RF. Magnetic resonance imaging of painful shoulder arthroplasty. J Shoulder Elbow Surg 2002;11:315–321
48. Goutallier D, Postel JM, Zilber S, Van Driessche S. Shoulder surgery: from cuff repair to joint replacement. An update. Joint Bone Spine 2003;70:422–432